Contribution from the Departamentos de Química Inorgánica, Universidad del País Vasco, Apdo. 644, 48080 Bilbao, Spain, and Universidad de Valencia, Valencia, Spain, Laboratoire de Chimie de Coordination du CNRS, Toulouse, France, and Laboratoire de Chimie du Solide du CNRS, Bordeaux, France

Structure, Dynamic Nuclear Magnetic Resonance Study, and Magnetic Properties of the Two Novel Chains $[Cu(paphy)X](PF_6)\cdot H_2O$ (paphy = Pyridine-2-carboxaldehyde 2-Pyridylhydrazone; X = Cl, Br). Synthetic Strategy of One-Dimensional Systems of Copper(II)

Teófilo Rojo,*,† José L. Mesa,† María I. Arriortua,† Jean M. Savariault,‡ Jean Galy,‡ Gerard Villeneuve,§ and Daniel Beltrán∥

Received March 11, 1988

A synthetic strategy of new one-dimensional systems of copper(II) with N-tridentate rigid planar ligands from monomeric complexes is described. The complexes $[Cu(paphy)X](PF_6)\cdot H_2O$ (paphy = pyridine-2-carboxaldehyde 2-pyridylhydrazone; X = Cl, Br) have been synthesized, and the crystal structures have been determined. The compounds crystallize in the monoclinic space group $P2_1/c$, with four molecules in a unit cell of dimensions a = 16.245 (6) Å, b = 15.731 (8) Å, c = 6.698 (2) Å, β = 99.19 (3)°, and V = 1689.7 (5) Å^3 and a = 16.484 (3) Å, b = 16.174 (3) Å, c = 6.593 (2) Å, β = 101.60 (3)°, and V = 1721.9 (3) Å^3 for the chlorine and bromine complexes, respectively. The structures have been refined by full-matrix least-squares techniques to final values of R = 0.076 (R_w = 0.102) and R = 0.059 (R_w = 0.078) based on 1687 and 1921 independent observations with $I \geq \sigma(I)$ and $I \geq 2\sigma(I)$, respectively. In both compounds, the $[Cu(paphy)X]^+$ unit is stacked in columns orientated in the |001| direction. In the stack, two successive copper complexes are in an alternating orientation. Such a disposition results from the formation of halogen bridges, building a linear chain when X = Cl and a ladderlike chain when X = Br. A disorder of the water molecule was found in each compound with a ratio of occupation in each site of 2:1 for O(1) and O(2), respectively. Reorientations of the PF_6 groups in the solid are discussed on the basis of ^{19}F NMR spectroscopic results. Magnetic susceptibility data have been measured in the temperature range 2-100 K. The single-chloride-bridged copper(II) chain compound exhibits ferromagnetic intrachain interactions with an exchange coupling constant of 0.63 cm^{-1}, while the ladderlike chain of bromide shows paramagnetic behavior in the temperature range studied. The estimation of exchange parameter using EPR spectroscopy for the bromide complex shows a $|J|$ value of 0.063 cm^{-1}. Magnetic and structural parameters of these complexes and the other μ-halo copper(II) chains are given, and some magneto-structural trends are discussed.

Introduction

The synthesis and analysis of low-dimensional magnetic systems is an area of strong interest to both physicists and chemists. Current research activity on the structural and magnetic properties of low-dimensional transition-metal compounds is aimed toward an understanding of the structural and chemical features that govern magnetic dimensionalities and the signs and magnitudes of exchange coupling constants.[1] Recent theoretical and experimental work has led to an understanding of the structural-magnetic correlations in simple binuclear species. In particular, it has been shown experimentally that the superexchange strength in the parallel square-planar dimers of copper(II) are related to the amount of distortion within the copper basal plane and to the distance of copper(II) to the apical atom in each pentacoordinate complex.[2-6]

A part of our research in this area is devoted to obtaining condensed systems of copper(II). In this way, we have established a synthetic strategy of new one-dimensional systems of copper(II) with tridentate ligands of general formula $[CuL_{III}XY]$ (L_{III} = tridentate ligand, X = coordinating anion, Y = coordinating or noncoordinating anion), which include bi- and polynuclear species.[4-7] In this work, we report the crystal structure and magnetic properties of two new μ-halo copper(II) chain compounds.

Experimental Section

Compound Preparations. Samples of $[Cu(paphy)X](PF_6)\cdot H_2O$ (X = Cl, Br) were prepared by addition of an excess of a KPF_6-saturated aqueous solution to both aqueous solutions (0.200 g in 30 mL) of $[Cu(paphy)X_2]$ (X = Cl, Br). The synthesis of the latter complexes has been previously described.[6,8] The resulting solutions were evaporated at room temperature to obtain crystals. These were isolated after filtration, washed with diethyl ether, and dried over P_2O_5 for 24 h. The crystals are green needles. Anal. Found (Calcd) for $C_{11}H_{12}OClPF_6CuN_4$ (I): C, 28.6 (28.7); N, 12.1 (12.2); H, 2.4 (2.6). Found (Calcd) for $C_{11}H_{12}OBrPF_6CuN_4$ (II): C, 26.1 (26.2); N, 11.0 (11.1); H, 2.3 (2.4).

Physical Measurements. The ^{19}F NMR study was carried out at 188 MHz, using a Bruker MSL 200 spectrometer. The absorption spectra were obtained by using a solid echo sequence (90°-τ-90°) with phase cycling followed by a Fourier transform. The temperature was controlled with a conventional gas-flow system blowing on the sample. The experimental second moments have been determined by numerical integration for the recordings of the absorption line. Magnetic susceptibility measurements were performed on powdered samples in the temperature range 2-100 K using a SQUID SHE magnetometer. Experimental susceptibilities were corrected for the diamagnetic contributions and for the TIP, estimated to be 60×10^{-6} cm^3 mol^{-1} per Cu(II) ion. A Bruker ER 200tt spectrometer equipped with a standard low-temperature device, operating at X-band calibrated by NMR probe for the magnetic field and a HP 5342A frequency counter for the microwave frequency, was used to record the EPR powder spectra of the complexes at different temperatures.

X-ray and Structure Determination. Crystals of $[Cu(paphy)Cl](PF_6)\cdot H_2O$ (I) and $[Cu(paphy)Br](PF_6)\cdot H_2O$ (II) as green needles were mounted in an Enraf-Nonius CAD4 automatic diffractometer with their long dimensions roughly parallel to the φ axis of the goniometer. The cell dimensions and orientation matrix were determined from the setting angles of 25 reflections with Mo Kα monochromated radiation. A fast data collection of reflections in the θ range 1-10° allowed us to choose the space group by looking at the systematic extinctions. A linear decay correction was applied to the data of compound II, which present a total loss of intensity of 1.3%. After absorption correction, the measured symmetry equivalent reflections were averaged. The structure was solved by using the Patterson heavy-tom method, and the remaining atoms were

* To whom correspondence should be addressed.
† Universidad del País Vasco.
‡ Laboratoire de Chimie de Coordination du CNRS.
§ Laboratoire de Chimie du Solide du CNRS.
∥ Universidad de Valencia.

(1) (a) Willett, R. D. *NATO ASI Ser., Ser. C* **1985**, *No. 140*, 389. (b) Hatfield, W. E. *Ibid.* **1985**, *No. 140*, 555. (c) Willett, R. D.; Landee, C. P. *J. Appl. Phys.* **1981**, *53*, 2004.
(2) Marsh, W. E.; Patel, K. C.; Hatfield, W. E.; Hodgson, D. J. *Inorg. Chem.* **1983**, *22*, 511.
(3) Landee, C. P.; Greeney, R. E. *Inorg. Chem.* **1986**, 25, 3771.
(4) Rojo, T.; Arriortua, M. I.; Ruiz, J.; Darriet, J.; Villeneuve, G.; Beltrán, D. *J. Chem. Soc., Dalton Trans.* **1987**, 285.
(5) Rojo, T.; Arriortua, M. I.; Mesa, J. L.; Cortés, R.; Villeneuve, G.; Beltrán, D. *Inorg. Chim. Acta* **1987**, *134*, 59.
(6) Mesa, J. L. Ph.D. Thesis, University of Basque Country, Bilbao, Spain, 1987.
(7) Folgado, J. V.; Coronado, E.; Beltrán, D.; Burriel, D.; Fuertes, A.; Miravitlles, C. *J. Chem. Soc., Dalton Trans.*, in press.
(8) Mesa, J. L.; Arriortua, M. I.; Lezama, L.; Pizarro, J. L.; Rojo, T.; Beltrán, D. *Polyhedron* **1988**, *7*, 1383.

0020-1669/88/1327-3904$01.50/0

Table I. Crystallographic Data for $[Cu(C_{11}H_{10}N_4)X](PF_6)\cdot H_2O$ (X = Cl, Br) Complexes

	I	II
chem formula	$CuClPF_6ON_4C_{11}H_{12}$	$CuBrPF_6ON_4C_{11}H_{12}$
a, Å	16.245 (6)	16.484 (3)
b, Å	15.731 (8)	16.174 (3)
c, Å	6.698 (2)	6.593 (2)
β, deg	99.19 (3)	101.60 (3)
V, Å^3	1689.7 (5)	1721.9 (3)
Z	4	4
fw	460.2	504.6
space group	$P2_1/c$ (No. 14)	$P2_1/c$ (No. 14)
T, °C	20	20
λ, Å	0.7107	0.7107
ρ_{obsd}, g cm^{-3}	1.81 (5)	1.88 (6)
ρ_{calcd}, g cm^{-3}	1.81	1.95
μ(Mo Kα), cm^{-1}	16.16	37.28
transmission coeff	0.71–0.97	0.66–0.90
$R(F)$	0.076	0.059
$R_w(F)$	0.102	0.078

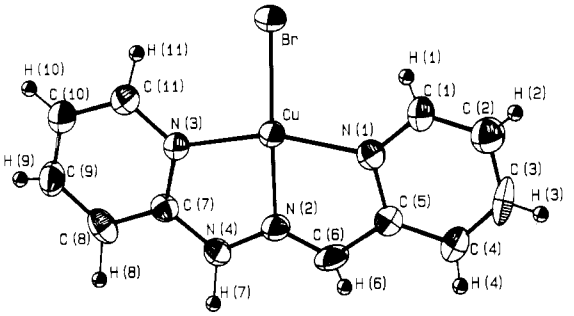

Figure 1. Perspective view of the $[Cu(paphy)Br]^+$ fragment with labeling of atoms. The thermal ellipsoids are drawn at the 50% probability level for the non-hydrogen atoms and with an arbitrary fixed radius for the hydrogen atoms. Except for the shape and dimensions of the thermal ellipsoids, the chlorinated complex is identical.

determined by alternating difference Fourier syntheses and least-squares refinements. A disorder of the water molecule was found in each compound with a ratio of occupation on each site of 2:1 for O(1) and O(2), respectively. Anisotropic thermal parameters were introduced for all non-hydrogen atoms except the oxygen atom O(2) of I, whose thermal parameter was kept isotropic. Only hydrogen atoms of the paphy moiety were included in refinements using C–H and N–H bond lengths of 0.95 Å and isotropic thermal parameters of 1.1 times the average values of the equivalent isotropic thermal contribution of the atoms they were attached to.

Crystallographic data for $[Cu(C_{11}H_{10}N_4)X](PF_6)\cdot H_2O$ (X = Cl, Br) compounds are reported in Table I.

Final positional and equivalent thermal parameters of $[Cu(paphy)X](PF_6)\cdot H_2O$ (X = Cl, Br) complexes are given in Table II.

Scattering factors and anomalous dispersion coefficients were taken from ref 9. All calculations were performed by using the Enraf-Nonius Structure Determination Package including ORTEP for drawings.[10] Further details are presented as supplementary material, together with thermal parameters, bond lengths and angles, mean average planes, and structure factors.

Results and Discussion

Synthetic Strategy of One-Dimensional Systems. The monomeric complexes of general formula $[CuL_{III}X_2]$ (L_{III} = tridentate ligand, X = halogen or pseudohalogen anion) show intermediate geometries between the trigonal bipyramid and square pyramid.[8,11-13] These compounds can be considered as intermediates in the synthesis of condensed systems. The synthetic strategy of these from the monomeric complexes involving a metathetic reaction is based on the equilibria

$$[Cu(L_{III})X_2](s) \rightleftarrows [Cu(L_{III})X_2](aq) \rightleftarrows [Cu(L_{III})X]^+(aq) + X^-(aq) \quad (1)$$

$$[Cu(L_{III})X]^+(aq) + Y^-(aq) \rightleftarrows (1/n)[Cu(L_{III})X]_n(Y)_n(aq \text{ or } s) \quad (2)$$

In eq 1 an X ligand is extruded while its charge is balanced by the noncoordinating Y anion, and in eq 2 the remaining X might now bridge two (dimers or simple chains) or three (ladderlike chains) metallic centers.

The $[Cu(L_{III})X]^+$ entities can be stabilized by the nature of the tridentate ligands (quasi-planar ligands) favoring the formation

Table II. Final Positional and Equivalent Thermal Parameters of $[Cu(paphy)X](PF_6)\cdot H_2O$ (X = Cl, Br) Complexes[a]

atom	x/a	y/b	z/c	B_{eq}, Å^2
	$[Cu(C_{11}H_{10}N_4)Cl](PF_6)\cdot H_2O$			
Cu	0.32425 (9)	0.3147 (1)	0.1474 (3)	3.18 (3)
Cl	0.3575 (2)	0.1833 (2)	0.2492 (6)	4.29 (8)
P	0.1560 (3)	0.5758 (4)	0.5467 (9)	7.2 (1)
F(1)	0.131 (1)	0.665 (1)	0.520 (3)	18.9 (7)
F(2)	0.2212 (8)	0.592 (1)	0.735 (2)	13.1 (5)
F(3)	0.0929 (9)	0.559 (1)	0.350 (3)	16.6 (6)
F(4)	0.0921 (8)	0.567 (1)	0.697 (3)	17.2 (6)
F(5)	0.171 (1)	0.482 (1)	0.567 (4)	20.9 (9)
F(6)	0.2249 (7)	0.586 (1)	0.415 (2)	13.5 (5)
O(1)	0.320 (1)	0.668 (1)	0.114 (3)	8.2 (6)
O(2)	0.252 (3)	0.750 (3)	0.337 (8)	7 (1)*
N(1)	0.2009 (6)	0.2977 (7)	0.069 (2)	3.9 (3)
N(2)	0.2906 (6)	0.4331 (6)	0.118 (2)	3.4 (2)
N(3)	0.4324 (6)	0.3726 (6)	0.229 (2)	3.5 (2)
N(4)	0.3512 (7)	0.4909 (7)	0.150 (2)	4.3 (3)
C(1)	0.1589 (8)	0.2259 (8)	0.045 (2)	3.7 (3)
C(2)	0.0733 (8)	0.2227 (9)	−0.009 (2)	4.5 (3)
C(3)	0.0332 (9)	0.298 (1)	−0.048 (3)	6.0 (4)
C(4)	0.073 (1)	0.375 (1)	−0.022 (3)	5.2 (4)
C(5)	0.1594 (8)	0.3715 (9)	0.034 (2)	4.1 (3)
C(6)	0.2141 (9)	0.4459 (9)	0.066 (2)	4.3 (3)
C(7)	0.4306 (8)	0.4577 (8)	0.211 (2)	3.7 (3)
C(8)	0.4998 (9)	0.5075 (9)	0.250 (2)	4.3 (3)
C(9)	0.5745 (8)	0.472 (1)	0.306 (2)	4.8 (3)
C(10)	0.5775 (7)	0.3848 (9)	0.331 (3)	4.9 (4)
C(11)	0.5070 (8)	0.3382 (9)	0.293 (3)	4.8 (4)
	$[Cu(C_{11}H_{10}N_4)Br](PF_6)\cdot H_2O$			
Br	0.35217 (6)	0.16803 (5)	0.1761 (2)	4.70 (2)
Cu	0.32032 (7)	0.30857 (6)	0.1602 (2)	4.02 (2)
P	0.1514 (2)	0.5701 (2)	0.5756 (6)	7.5 (1)
F(1)	0.1340 (9)	0.6629 (6)	0.570 (2)	15.8 (5)
F(2)	0.2212 (5)	0.5790 (8)	0.768 (1)	13.7 (4)
F(3)	0.0873 (7)	0.5632 (8)	0.372 (2)	17.2 (4)
F(4)	0.0871 (6)	0.5631 (8)	0.713 (2)	16.8 (4)
F(5)	0.1574 (7)	0.4760 (5)	0.580 (2)	16.3 (5)
F(6)	0.2212 (5)	0.5801 (8)	0.455 (1)	13.4 (3)
O(1)	0.3326 (8)	0.6475 (6)	0.168 (2)	6.0 (3)
O(2)	0.251 (1)	0.750 (1)	0.377 (4)	5.4 (5)
N(1)	0.1966 (5)	0.2977 (5)	0.099 (1)	4.5 (2)
N(2)	0.2907 (4)	0.4240 (4)	0.146 (1)	4.0 (2)
N(3)	0.4322 (4)	0.3597 (4)	0.215 (1)	3.7 (2)
N(4)	0.3549 (5)	0.4777 (4)	0.178 (1)	4.4 (2)
C(1)	0.1497 (6)	0.2300 (6)	0.076 (2)	5.2 (3)
C(2)	0.0661 (7)	0.2320 (7)	0.034 (2)	6.0 (3)
C(3)	0.0289 (6)	0.3061 (8)	0.015 (2)	7.5 (3)
C(4)	0.0729 (6)	0.3777 (7)	0.036 (2)	6.4 (3)
C(5)	0.1575 (6)	0.3729 (6)	0.080 (1)	4.5 (2)
C(6)	0.2152 (6)	0.4406 (5)	0.108 (2)	5.2 (2)
C(7)	0.4310 (5)	0.4422 (5)	0.215 (1)	3.6 (2)
C(8)	0.5026 (6)	0.4895 (6)	0.252 (1)	4.9 (2)
C(9)	0.5768 (6)	0.4487 (7)	0.288 (2)	5.1 (2)
C(10)	0.5795 (6)	0.3659 (6)	0.289 (2)	5.1 (2)
C(11)	0.5061 (6)	0.3201 (6)	0.255 (2)	4.7 (2)

[a] The starred value indicates that the atom was refined isotropically. Anisotropically refined atoms are given in the form of the isotropic equivalent thermal parameters defined as $^4/_3[a^2\beta_{11} + b^2\beta_{22} + c^2\beta_{33} + 2ab(\cos\gamma)\beta_{12} + 2ac(\cos\beta)\beta_{13} + 2bc(\cos\alpha)\beta_{23}]$.

(9) Cromer, D. T.; Waber, J. T. *International Tables for X-Ray Crystallography*; Kynoch: Birmingham, England, 1974; Vol. IV, Table 2.2B.
(10) Frenz, B. A. *The Enraf-Nonius CAD4 SDP*; Schenk, H.; Olthof-Hazelkamp, R., van Konigsveld, H., Bassi, G. G., Eds.; Delft University Press: Delft, Holland, 1978; p 64.
(11) Rojo, T.; Vlasse, M.; Beltrán, D. *Acta Crystallogr.* **1983**, *C39*, 194.
(12) Rojo, T.; Mesa, J. L.; Arriortua, M. I.; Beltrán, D. *An. Quim.* **1984**, *80B*, 477.
(13) Arriortua, M. I.; Mesa, J. L.; Rojo, T.; Debaerdemaeker, T.; Beltrán-Porter, D.; Stratemeier, H.; Reinen, D. *Inorg. Chem.* **1988**, *27*, 2976.

Table III. Selected Bond Distances (Å) and Angles (deg) for $[Cu(C_{11}H_{10}N_4)X](PF_6)\cdot H_2O$ (X = Cl, Br) Complexes[a]

dist/angle	X = Cl	X = Br	dist/angle	X = Cl	X = Br
Cu–X	2.217 (4)	2.331 (1)	Cu–X′	2.805 (4)	3.358 (2)
Cu–X″	3.980 (4)	3.358 (2)	Cu–N(1)	2.01 (1)	2.005 (8)
Cu–N(2)	1.94 (1)	1.927 (7)	Cu–N(3)	1.98 (1)	1.986 (7)
Cu–Cu′	3.919 (3)	3.802 (2)	Cu–X–Cu′	102.0 (2)	81.72 (5)
X–Cu–N(1)	98.1 (3)	97.7 (2)	X–Cu–N(2)	167.6 (4)	178.4 (2)
X–Cu–N(3)	100.5 (3)	101.8 (2)	X–Cu–X′	103.2 (1)	94.36 (5)
X–Cu–X″	73.1 (1)	94.38 (5)	X′–Cu–N(1)	95.0 (4)	99.6 (3)
X′–Cu–N(2)	89.1 (3)	85.9 (2)	X′–Cu–N(3)	87.7 (4)	79.1 (2)
X′–Cu–X″	161.31 (9)	158.07 (4)	N(1)–Cu–N(2)	81.2 (4)	80.7 (2)
N(2)–Cu–N(3)	79.0 (4)	79.8 (2)	N(1)–Cu–N(3)	160.1 (4)	160.4 (3)
N(2)–C(6)	1.25 (2)	1.25 (1)	N(2)–N(4)	1.33 (1)	1.352 (9)
N(4)–C(7)	1.39 (2)	1.36 (1)	C(5)–C(6)	1.46 (2)	1.44 (1)
N(4)–H(7)	0.9 (1)	1.1 (1)	C(6)–H(6)	0.8 (1)	0.76 (9)
N(1)–C(5)–C(6)	113 (1)	112.1 (8)	C(5)–C(6)–N(2)	118 (1)	118.0 (8)
C(6)–N(2)–N(4)	128 (1)	127.6 (7)	N(2)–N(4)–C(7)	115 (1)	115.0 (7)
N(4)–C(7)–N(3)	114 (1)	115.9 (7)			
O(1)···N(4)	2.83 (2)	2.77 (1)	O(1)–O(2)	2.37 (6)	2.68 (2)
O(2)···F(1)	2.82 (5)	2.88 (3)	O(2)···F(6)	2.69 (6)	2.85 (2)
O(2)···F‴(1)	2.97 (5)	2.87 (2)	O(2)···F‴(2)	2.60 (5)	2.88 (2)
P–F(1)	1.46 (2)	1.53 (1)	P–F(2)	1.53 (1)	1.538 (7)
P–F(3)	1.56 (2)	1.54 (1)	P–F(4)	1.56 (2)	1.53 (1)
P–F(5)	1.50 (2)	1.525 (9)	P–F(6)	1.54 (1)	1.533 (9)
F(1)–F(2)	2.21 (2)	2.20 (1)	F(1)–F(3)	2.06 (2)	2.12 (2)
F(1)–F(4)	2.10 (2)	2.09 (2)	F(1)–F(5)	2.96 (2)	3.05 (1)
F(1)–F(6)	2.17 (2)	2.21 (2)	F(2)–F(3)	3.09 (2)	3.07 (1)
F(2)–F(4)	2.11 (2)	2.18 (2)	F(2)–F(5)	2.15 (2)	2.21 (1)
F(2)–F(6)	2.16 (2)	2.06 (1)	F(3)–F(4)	2.33 (3)	2.25 (2)
F(3)–F(5)	2.14 (2)	2.14 (1)	F(3)–F(6)	2.16 (2)	2.18 (1)
F(4)–F(5)	2.13 (3)	2.12 (2)	F(4)–F(6)	3.10 (2)	3.06 (1)
F(5)–F(6)	2.18 (2)	2.23 (1)			

[a] Position of atom X′ = position of atom X after $x, {}^1/_2 - y, z - {}^1/_2$. [b] Position of atom X″ = position of atom X after $x, {}^1/_2 - y, {}^1/_2 + z$. [c] Position of atom X‴ = position of atom X after $x, {}^3/_2 - y, z - {}^1/_2$.

of condensed systems when X is a potentially bridging anion.[4,5,14,15] Likewise, when L_{III} is an anionic tridentate ligand (bpca = *N*-(2-pyridinylcarbonyl)-2-pyridinecarboximidate) the formation of neutral $[Cu(L_{III})X]$ entities has been observed.[7,16] In these cases, both the "quasi-planarity" of bpca and the tendency of copper(II) to acquire a "4+1" coordination mode would favor the stacking of [Cu(bpca)X] units to give dimers or chain structures.[7]

Structure. The X-ray crystal structures of the title compounds both consist of $[Cu(paphy)X]^+$ and PF_6^- ions and of water molecules. The copper complex, presented with labeling in Figure 1, is stacked in columns orientated in the |001| direction.

In the stack, two successive copper complexes are in alternating orientation. The corresponding Cu–X orientations make angles of 146.4 (9)° (X = Cl) and 153.2 (7)° (X = Br). Their average planes are nearly parallel [angle of 10.4 (5)° for X = Cl and 0.1 (3)° for X = Br] and halfway up the *c* length. Such a disposition results from the formation of halogen bridges building a linear chain when X = Cl and a ladderlike chain when X = Br. Figures 2 and 3 show the skeleton and stereoscopic view of these chains, respectively. So far the ladderlike chain of copper(II) has been found only in four complexes,[17-19] and it may be noticed that the *c* cell dimensions are similar in each compound [6.372 (13),[17] 6.208 (3),[17] 6.859 (1),[18] 6.267 (3),[19] and 6.593 (2) Å for the ladderlike chain of the title compound].

Between these columns and in the average plane of the paphy ligand lie the PF_6 ions: the distance of the phosphorus atoms to the average plane is 0.515 (6) Å (X = Cl) and 0.009 (4) Å (X = Br). The first water molecule O(1), with a site occupation of ${}^2/_3$, makes a hydrogen bond with the N(4) atom and is in the average plane as well [0.20 (2) Å (X = Cl) and 0.01 (1) Å (X = Br)]. The second water molecule O(2), with a site occupation of ${}^1/_3$, is located in the middle plane of two successive PF_6 groups and makes hydrogen bonds between the F(1) and F(6) fluorine atoms of one PF_6 and F‴(1) and F‴(2) fluorine atoms of a second PF_6 located at $x, {}^3/_2 - y, z - {}^1/_2$ from the first one.

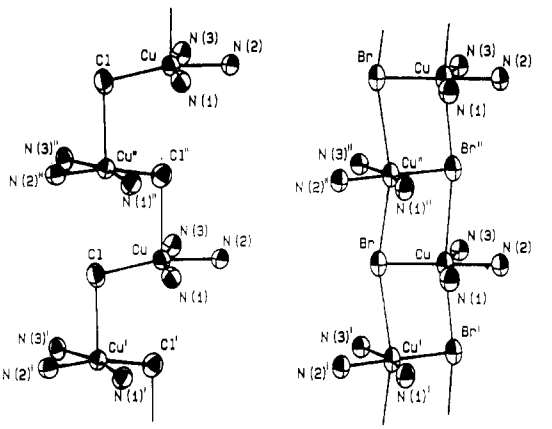

Figure 2. Perspective view of the chaining up of the $[Cu(paphy)X]^+$ (X = Cl, Br) ions in the |001| direction. The thermal ellipsoids are as in Figure 1.

Except for the halogen part, both complexes are identical. Table III gathers the bond distances and angles pertinent to the discussion.

The paphy ligands are planar with the conformation of the tridentate ligand [N(1),N(2),N(3)] found in earlier studies.[20-22]

(14) Folgado, J. V.; Coronado, E.; Beltrán, D. *J. Chem. Soc., Dalton Trans.* **1986**, 1061.
(15) Folgado, J. V.; Escrivá, E.; Beltrán, A.; Beltrán, D. *Transition Met Chem. (London)* **1986**, *11*, 485.
(16) Folgado, J. V.; Escrivá, E.; Beltrán, A.; Beltrán, D. *Transition Met. Chem. (London)* **1987**, *12*, 306.
(17) Helis, H. M.; Goodman, W. H.; Wilson, R. B.; Morgan, J. A.; Hodgson, D. J. *Inorg. Chem.* **1977**, *16*, 2412.
(18) Brown, D. B.; Donner, J. A.; Hall, J. W.; Wilson, S. R.; Wilson, R. B.; Hodgson, D. J.; Hatfield, W. E. *Inorg. Chem.* **1979**, *18*, 2635.
(19) Endres, H. *Acta Crystallogr.* **1983**, *C39*, 1192.
(20) Casey, A. T.; Hoskins, B. F.; Traverso, I. P. *Aust. J. Chem.* **1984**, *37*, 739.
(21) Gerloch, M. *J. Chem. Soc. A* **1966**, 1317.
(22) Barianak, E.; Bruce, R. S.; Freman, H. C.; Grath, B. G. *Inorg. Chem.* **1974**, *13*, 1032.

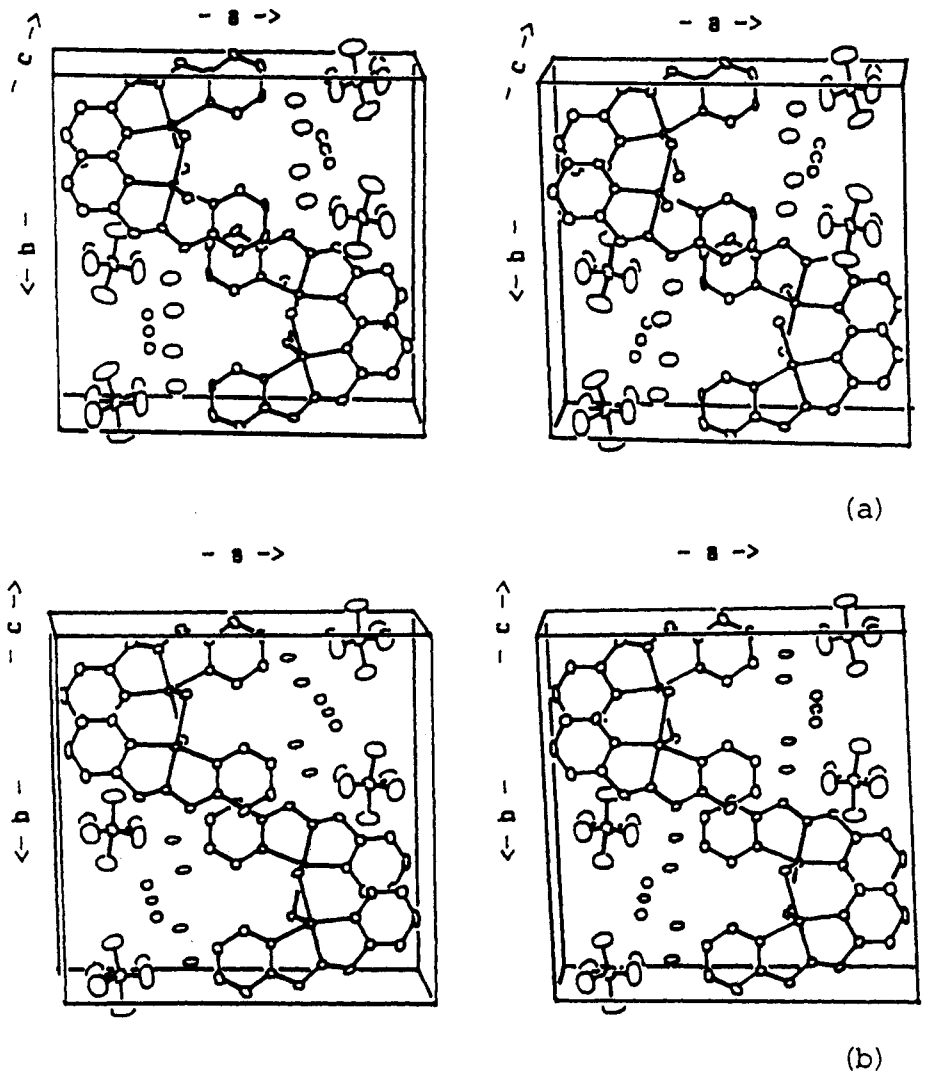

Figure 3. Stereoscopic view of the cell of $[Cu(paphy)X](PF_6)\cdot H_2O$ complexes: (a) X = Cl; (b) X = Br.

The comparison with the Pd,[20] Co,[21] and Yb[22] complexes shows that the main distortions appear in the hydrazine residue. The C(6)–N(2) distances are shorter than those found in the Pd[20] or Co[21] compounds by 0.05 (2) Å and are of the same order of magnitude as the distance that is present in the isolated paphy molecule.[20] The largest modifications occur with the angles N(1)–C(5)–C(6), C(5)–C(6)–N(2), C(6)–N(2)–N(4), N(2)–N(4)–C(7), and N(4)–C(7)–N(3), with average deviations equal to −3.7, +3.9, +5.0, +2.9, and −2.8°, respectively. These variations can be interpreted as a stretching of the chain C(5)–C(6)–N(2)–N(4)–C(7) in association with the pinching of the two extreme angles, while the N(1)···N(3) distance is kept nearly constant.

The surroundings of the copper atom are different in the chlorinated and in the brominated compounds. This difference can be assigned to the stacking of the complex ions $[Cu(paphy)X]^+$ in the crystals, a linear chain for the chlorine compound and a ladderlike chain for the bromine one, which correspond to a five- and a six-coordinate type, respectively. In the chlorine-substituted compound, the deformations toward the square pyramid are similar to those observed in the Co compound although the Cu–Cl distance [2.805 (4) Å] is much greater than the Co–Cl one [2.328 (4) Å]. The copper atom is pulled out from the plane of the paphy ligand toward the chlorine atom of the upper complex by 0.109 (2) Å, while the chlorine atom is drawn toward the copper atom of the lower complex by 0.214 (4) Å.

A determination of the distortion of the polyhedron formed, according to Muetterties' method[23] completed by the model of the rigid sphere proposed by Kouba[24] and the geometric dimensions collected by Hathaway[25] in the copper chemistry, is reported in Table IV. As expected, the shape of the polyhedron is close to the regular square pyramid with a deformation of 30% to the trigonal bipyramid. But this evaluation is only a trend because the angles of the faces of the polyhedron do not follow Berry's

Table IV. Deformation of the Coordination Polyhedron (Angles in deg) of the Five-Coordinate Copper(II) Ion in the Chlorinated Complex I Compared to the Ideal Trigonal Pyramid (TBP) and the Regular Square Pyramid (SP_r)[a]

dihedral angle	TBP	I	SP_r
Cl′–Cl–N(1)–N(2)	101.5	111.7	121.8
Cl′–N(1)–N(2)–Cl	101.5	117.7	121.8
Cl′–N(2)–N(3)–Cl	101.5	108.3	121.8
Cl′–N(3)–Cl–N(2)	101.5	112.6	121.8
Cl–Cl′–N(1)–N(2)	53.1	86.6	73.9
Cl–Cl′–N(3)–N(2)	53.1	81.7	73.9
N(1)–Cl′–Cl–N(3)	101.5	69.3	73.9
N(1)–Cl′–N(2)–N(3)	101.5	79.3	73.9
N(1)–Cl–N(2)–N(3)	53.1	7.8	0.0
Δ	0	0.70	1

[a] $\Delta = \sum(\delta q_{i,exp} - \delta q_{i,TBP})/(\delta q_{i,SP_r} - \delta q_{i,TBP})$. The Cl′ atom is taken as the apex of the Sp_r, which corresponds to an equatorial position of the TBP. The N(1) and N(3) atoms define the axial orientation of the TBP. The position of atom Cl′ = position of atom Cl after x, $^1/_2 - y$, $z - ^1/_2$ (see Table II).

(23) Muetterties, E. L.; Guggenberger, L. J. *J. Am. Chem. Soc.* **1974**, *96*, 1748.
(24) Kouba, J. K.; Wreford, S. S. *Inorg. Chem.* **1976**, *15*, 1463.
(25) Hathaway, B. J. *Coord. Chem. Rev.* **1982**, *41*, 423.

pathway.[26] Nevertheless, a similar result is obtained when Kepert's model, which is based on an interligand repulsion approach, is applied.[8,27]

The ladderlike chain of the brominated compound implies a surrounding of the copper atom of the elongated-octahedron type, with axial Cu–Br′ bonds $\simeq 1$ Å greater than the equatorial ones. Such a deformation has been observed in several examples of copper halide oligomers that stack together to form alternating chains.[28,29] For the ladderlike chains, the deviation of the coordination polyhedron from the octahedral geometry considering the trigonal prismatic as limit geometry was calculated by quantification of Muetterties' method.[23,30] The value thus obtained for the title compound, 9% ($\Delta = 0.09$), is similar to those for the (2-(aminomethyl)pyridine)copper(II) ($\Delta = 0.09$), hydrazinium trichlorocuprate(II) ($\Delta = 0.09$), and dichloro(oxamide dioxime)copper(II) ($\Delta = 0.08$) complexes and higher than that for the (2-methyl-1,2-diaminopropane)copper(II) compound, 4% ($\Delta = 0.04$) (supplementary material).

In both stackings the paphy ligands are not exactly in alternate orientations, and one of the final pyridyl groups overlaps. The resulting interaction consists of a repulsive force that is applied on this part of the paphy ligand. The distance between two successive complexes being of the same order [3.32 (3) Å], the intensity of this force can be considered as constant in both compounds. The formation of the halogen bridge corresponds to an attractive force that draws the complexes toward each other. Because these two forces are not applied at the same point in the complex, the corresponding torque tends to rotate the complex with an amplitude that depends on the relative intensity of each force.

In the chlorinated compound, the angle of two successive complexes is equal to 10.4 (5)°, which indicates a strong attraction due to the formation of the halogen bridge: the Cu–Cl distance is shorter than the step of the stacking by about 0.52 Å. Nevertheless, this distance is similar to that found in the ladderlike chain of hydrazinium trichlorocuprate(II) [2.856 (1) Å],[18] where no repulsion between ligands is observed and where the coordination planes are parallel. To this break in the parallelism of the paphy Cl complex corresponds a divergence of the two halogen bridges of the ladderlike chain to form a zigzag chain.

In the brominated compound, the complexes being parallel in the stack, the attractive interaction is very weak. But the comparison with the similar ladderlike chain dibromo[2-(aminomethyl)pyridine]copper(II)[17] shows differences that can be explained by the interaction between the ligands as mentioned above: The Cu–Br′ distance is larger than that observed in ref 17 by $\simeq 0.1$ Å, and the Cu, Br, Cu′, and Br′ atoms are not planar.

All these modifications show that the interaction between ligands plays an important role in the formation of the particular stacking of the complexes.

The high values of the fluorine thermal parameters (see Table II and Experimental Section) indicate the existence of an important mobility of these atoms. This dynamic state, observed in other compounds with PF_6^- ions,[4,31] can be studied from the analysis of the thermal variation of the ^{19}F nuclear magnetic resonance (NMR) absorption line width.

NMR Study of Fluorine Reorientation in the PF_6^- Anion of the [Cu(paphy)Cl](PF_6)·H_2O Complex. The variation of the line widths (expressed in frequency units) of the ^{19}F spectra in the temperature range 100–300 K is shown in Figure 4. The experimental second moment (Hz^2) is obtained by eq 3, where ν_0

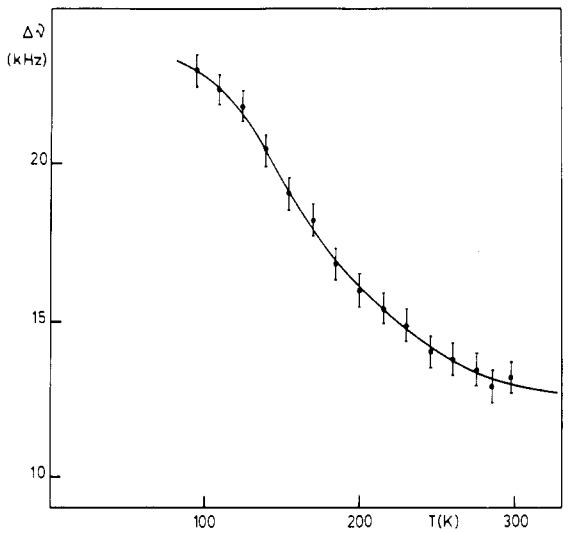

Figure 4. Variation of the line width of the ^{19}F absorption line.

Table V. Contribution to the Second Moment (in G^2) of the ^{19}F Line Calculated for a Spherical Rotation of the PF_6^- Group

	interaction						
	F–F	F–P	F–Cu	F–N	F–Cl	F–H	total
M_2	0.0120	0.0022	0.0030	0.0009	0.0004	<0.2	<0.22

$$M_2 = \int_0^\infty (\nu - \nu_0)^2 f(\nu)\, d\nu \qquad (3)$$

indicates the position of the gravity center of the absorption line and $f(\nu)$ the normalized signal at ν frequency. Usually, its value is expressed in magnetic field units [M_2 (Hz^2) = $\hat{\gamma}^2 M_2$ (G^2), where $\hat{\gamma} = \gamma/2\pi$]. The experimental second moment decreases from 8.63 G^2 (100 K) to 2.44 G^2 (300 K).

The theoretical second moment produced by magnetic dipole–dipole interactions can be calculated from Van Vleck's treatment of a rigid lattice.[32] For a polycrystalline sample, it may be written as eq 4, where indices "i" and "j" refer to the nuclei giving rise to the absorption concerned and "k" refers to other magnetic nuclei in the material, "I" is the nuclear spin, "$\hat{\gamma}$" is the gyromagnetic ratio, "N" is the number of resonant nuclei, and "r_{ij}" and "r_{ik}" are the internuclear distances.

$$M_2 = {}^3/_5[\hat{\gamma}_i^2 \hbar^2 I_i(I_i + 1) N^{-1} \sum_{ij} r_{ij}^{-6}] + {}^4/_{15}[\hbar^2 N^{-1} \sum_{ik} \hat{\gamma}_k^2 I_k(I_k + 1) r_{ik}^{-6}] \qquad (4)$$

The dipole–dipole broadening of the line is due to intragroup interactions (F–F and F–P) for the PF_6^- ion and also to the interactions with all the other magnetic nuclei (F and P located in the other PF_6^- ions, Cu, N, Cl, H). We call the latter "intergroup" or "extra" interactions.

The intragroup contribution to the second moment considering the interatomic distances given in Table III can be calculated by using eq 4. The value thus obtained is M_2(intra) = 15.30 G^2 (13.22 G^2 for the F–F interactions and 2.08 G^2 for the F–P ones). It is approximately 2 and 6 times higher than the experimental values at 100 and 300 K, respectively. These results indicate that the PF_6^- ions have a dynamic behavior even at temperatures as low as 100 K. Two possible mechanisms to explain the mobility of PF_6^- ions are the spherical rotation and the reorientations of the PF_6^- groups around a symmetry axis.

Spherical Rotation. In this model the PF_6 group is assimilated to a sphere that reorientates itself at random around a continuous range of axes. As a consequence the intragroup interactions

(26) Berry, R. S. *J. Chem. Phys.* **1960**, *32*, 933.
(27) (a) Kepert, D. L. *Inorg. Chemistry Concepts, Inorganic Stereochemistry*; Springer-Verlag: New York, 1982; Vol. VI. (b) Favas, M. C.; Kepert, D. L. *Prog. Inorg. Chem.* **1980**, *27*, 325. (c) Kepert, D. L.; Kucharsky, E. S.; White, A. H. *J. Chem. Soc., Dalton Trans* **1980**, 1932.
(28) (a) Geiser, U.; Willett, R. D.; Lindbeck, M.; Emerson, K. *J. Am. Chem. Soc.* **1986**, *108*, 1173. (b) Geiser, U.; Gaura, R. H.; Willett, R. D.; West, D. X. *Inorg. Chem.* **1986**, *25*, 4203.
(29) Landee, C. P. *NATO ASI Ser., Ser. B* **1987**, *No. 168*, 75.
(30) Cortés, R.; Arriortua, M. I.; Rojo, T.; Solans, X.; Miravitlles, C.; Beltrán, D. *Acta Crystallogr.* **1985**, *C41*, 1733.
(31) Arriortua, M. I.; Rojo, T.; Amigó, J. M.; Germain, G.; Declercq, J. P. *Acta Crystallogr.* **1982**, *B38*, 1323.
(32) Van Vleck, J. H. *Phys. Rev.* **1948**, *711*, 168.

Table VI. Second Moment (in G^2) of the ^{19}F Line Calculated for a Rotation of the PF_6^- Group around a Single Axis

axis C_i	contribn F–F	contribn P–F	total
C_2	2.83	0.26	3.09
C_3	3.11	0	3.11
C_4	1.76	1.02	2.78

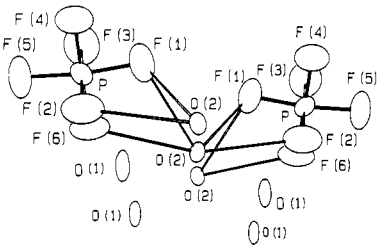

Figure 5. Representation of the PF_6^- anion and O(1) and O(2) atoms along the c axis.

average out to zero and we are left with the "extra" or "intergroup" interactions (i.e., PF_6–PF_6, F–Cu, F–N, F–Cl, and F–H). McCall and Douglas[33] have shown that for spherical rotation the intergroup interactions are equivalent to the rigid lattice values obtained by placing each nucleus at the center of the sphere, in our case at the phosphorus positions. Then, from the knowledge of the atomic positions and Van Vleck's relation, it is easy to calculate all the different contributions to the second moment. Table V gives the results obtained. The F–H contribution has not been calculated because the proton positions are unknown. This contribution has been estimated by considering a minimum distance of 3 Å between the F and O(2) atoms, which are joined by hydrogen bonds. The calculated value (see Table V) is 10 times lower than the observed one [M_2 = 2.44 G^2 (300 K)]. Therefore, the spherical rotation model does not describe the dynamic behavior of the PF_6^- ion.

Reorientations around a Symmetry Axis. The simplest motions that could narrow the fluorine resonance line are reorientations of the PF_6^- groups about the (pseudo) 2-, 3-, and 4-fold symmetry axes. For such a mechanism the second moment would be reduced by the factor $^1/_4(3\cos^2\nu_{ij} - 1)^2$, where ν_{ij} is the angle between the internuclear vector r_{ij} and the rotation axis. Table VI gives the relative intragroup contributions to the ^{19}F second moment of the F–F interactions in the three cases.

The experimental value at 300 K (ΔM_2 = 2.44 G^2) corresponds well to the calculated ones (see Table VI). It suggests that the PF_6^- ions are reorientated around a symmetry axis at this temperature. Nevertheless, the accuracy of the experimental data and the similar calculated values prevent assigning the rotation to a specific axis.

In Figure 4 a progressive increase of the second moment can be observed when the temperature has been reduced to 100 K. It shows a restriction in the motion of PF_6^- groups which do not obtain the treatment of a rigid lattice at this temperature. The evolution of the line width of the ^{19}F absorption line follows Arrhenius's law with the value of the activation energy 6×10^{-2} eV. (This indicates the energetic barrier that hinders the rotation around a symmetry axis.)

A similar study has been realized in the $[Cu(terpy)Cl]_2(PF_6)_2$ complex (terpy = 2,2′:6′,2″-terpyridine), where the PF_6^- ions act as counterions.[4] In this case, the experimental fluorine second moment shows a constant value (0.96 G^2) within the temperature range 200–450 K, corresponding to spherical rotation of PF_6^- ions. In our case, the restriction motion can be reasonably ascribed to F···O(2) hydrogen bonding (Figure 5). With this hypothesis the water molecule would be delocalized over the O(1) and O(2) positions.

Magnetic Behavior. The study of magnetic susceptibility data within the temperature range 2–100 K shows different magnetic behavior for both compounds. The $[Cu(paphy)Br](PF_6)\cdot H_2O$ complex exhibits a paramagnetic behavior in all temperature ranges. However, ferro- or antiferromagnetic interactions with exchange coupling constants of $|J| < 0.1$ cm^{-1} (0.14 K) can only be detected at temperatures lower than 2 K.

Table VII. Values Obtained by Simulation of the X-Band EPR Spectra of the $[Cu(paphy)X](PF_6)\cdot H_2O$ (X = Cl, Br) Complexes

compd	$g_\parallel$	$g_\perp$	$\bar{g}$	$\Gamma_\parallel$, G	$\Gamma_\perp$, G
$[Cu(paphy)Cl](PF_6)\cdot H_2O$	2.200	2.045	2.097	115	70
$[Cu(paphy)Br](PF_6)\cdot H_2O$	2.280	2.050	2.127	270	390

A plot of $1/\chi_M$ versus T for the $[Cu(paphy)Cl](PF_6)\cdot H_2O$ complex (Figure 6) reveals Curie–Weiss behavior for $T > 30$ K with a positive temperature intercept of 6 K. The slope corresponds to a Curie constant of 0.43 emu mol^{-1} K). The plot of $\chi_M T$ versus T (Figure 7) shows a constant value of $\chi_M T$ when cooling down from 100 K to about 30 K. For lower tempratures the data rise indicates an increase of effective moment caused by ferromagnetic coupling within Cu(II) ions. These magnetic data may be described by the series expansion for the Heisenberg model ($H = -2J\sum_i S_i S_{i+1}$) for ferromagnetically coupled $S = {}^1/_2$ ions that was derived by Baker and co-workers.[34] The expansion is given as eq 5, where $x = 2|J|/KT$. Nevertheless, the best fit

$$\chi = [N\langle g\rangle^2\beta^2/4KT][1 + Ax + Bx^2 + Cx^3 + Dx^4 + Ex^5/1 + A'x + B'x^2 + C'x^3 + D'x^4]^{2/3} \quad (5)$$

$$A = 5.7979916 \qquad A' = 2.7979916$$

$$B = 16.902653 \qquad B' = 7.0086780$$

$$C = 29.376885 \qquad C' = 8.6538644$$

$$D = 29.832959 \qquad D' = 4.5743114$$

$$E = 14.036918$$

(Figure 7) is obtained by considering antiferromagnetic interchain interactions (j) which modify the magnetic susceptibility expression (χ) by eq 6, where Z is the number of nearest neighbors in the

$$\chi' = \chi/[1 - (2Zj\chi/N\langle g\rangle^2\beta^2)] \quad (6)$$

adjacent chains (in this case $Z = 4$). The parameters used for the fit are the following: $J = 0.63$ cm^{-1}, $j = -0.06$ cm^{-1}, and $g = 2.18$.

Magnetization measurements at 2 K and applied magnetic fields up to 60 kG are reported in Figure 8 for the two compounds under discussion. Likewise, the theoretical variation of magnetization for a paramagnetic compound is plotted. Several conclusions can be obtained from the magnetization curves. (i) There is a linear variation with the applied magnetic fields up to 5 and 10 kG for the chlorine and bromine complexes, respectively. The last value is similar to the maximum one observed on the paramagnetic compounds. (ii) The bromide compound exhibits a curve similar (allowing for experimental errors) to the paramagnetic ones. Therefore, the ladderlike chain will show very weak magnetic coupling. (iii) The magnetization curve of the linear chain appears higher than the other ones and changes toward saturation in magnetic fields higher than 20 kG, showing ferromagnetic interactions.

The powder EPR spectrum of the chloride complex is characteristic of a tetragonal structure with $g_\parallel = 2.193$ and $g_\perp = 2.050$ (Figure 9a). These values remain nearly unchanged at 4 K ($g_\parallel = 2.191$, $g_\perp = 2.052$). For the bromide complex the EPR spectrum shows a large line width, which does not allow a good resolution of the g tensor (see Figure 9b). The EPR absorption lines in both compounds have Lorentzian shapes; therefore, it is possible to obtain the g and Γ (half-width at half-height) values by simulation of the spectra. The values thus obtained are shown in Table VII (the simulation of the spectrum for the bromide

(33) McCall, D. W.; Douglas, D. C. *J. Chem. Phys.* **1960**, *33*, 777.

(34) Baker, G. A.; Rushbrooke, G. S.; Gilbert, H. E. *Phys. Rev.* **1964**, *135*(5A), 1272.

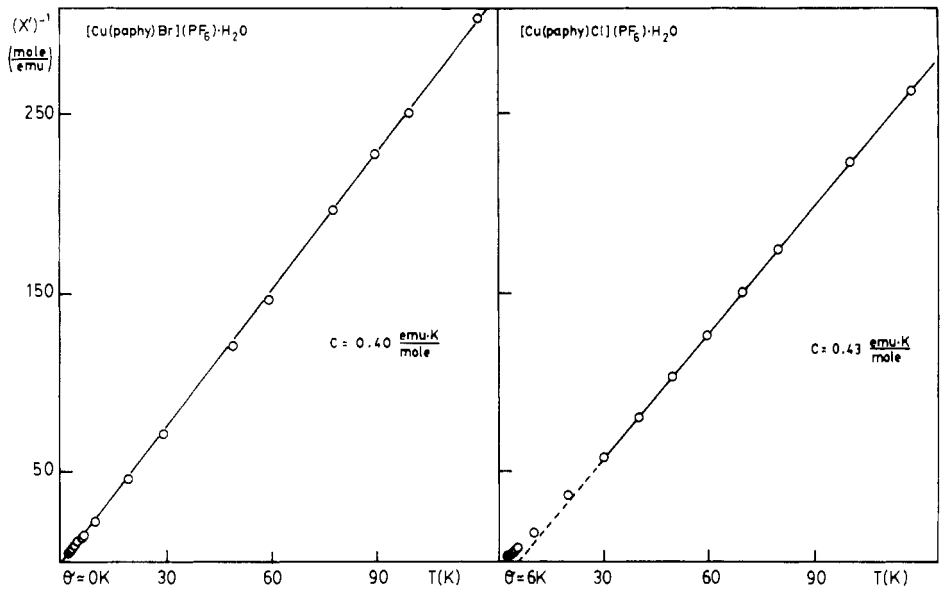

Figure 6. Temperature dependence of the inverse susceptibility for $[Cu(paphy)X](PF_6)\cdot H_2O$ (X = Cl, Br) complexes.

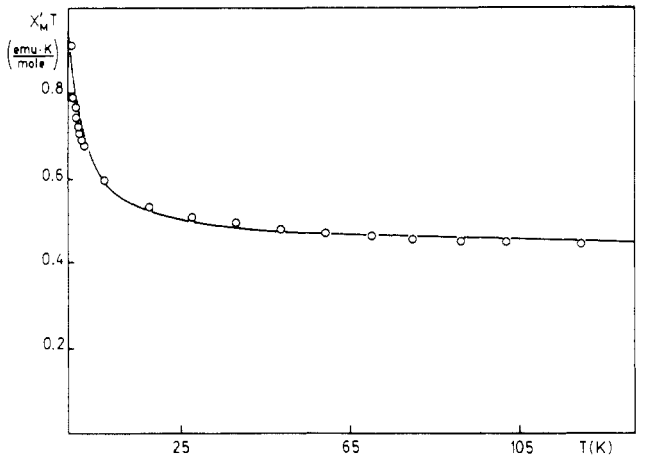

Figure 7. Plot of $\chi'_M T$ versus temperature for the $[Cu(paphy)Cl](PF_6)\cdot H_2O$ complex. The solid line is the best fit of the ferromagnetic Heisenberg chain model considering also interchain interactions to the experimental data with $J = 0.63$ cm^{-1}, $j = -0.06$ cm^{-1}, and $g = 2.18$.

complex has been performed by considering the g values of the chloride compound).

Estimation of the Exchange Parameter (J) Using EPR Spectroscopy. Application to $[Cu(paphy)Br](PF_6)\cdot H_2O$. In the concentrated magnetic systems the line width and the line shape are governed by two effects. The increase of the line width toward the Gaussian shape is produced by the dipolar interactions. On the other hand, the occurrence of exchange coupling causes a narrowing of the line whose shape becomes Lorentzian. The J value in the ladderlike chain under discussion estimated from magnetic susceptibility is lower than 0.1 cm^{-1}. Owing to the fact that $J \ll g\beta H$, only the secular ($\Delta M = 0$) terms contribute to the second moment of the EPR absorption line, which is expressed in frequency units as[35-37]

$$M_2 = {}^3/_4[S(S+1)\langle g\rangle^4\beta^4/h^2]\sum_k r_K^{-6}(3\cos^2\vartheta_K - 1)^2 \quad (7)$$

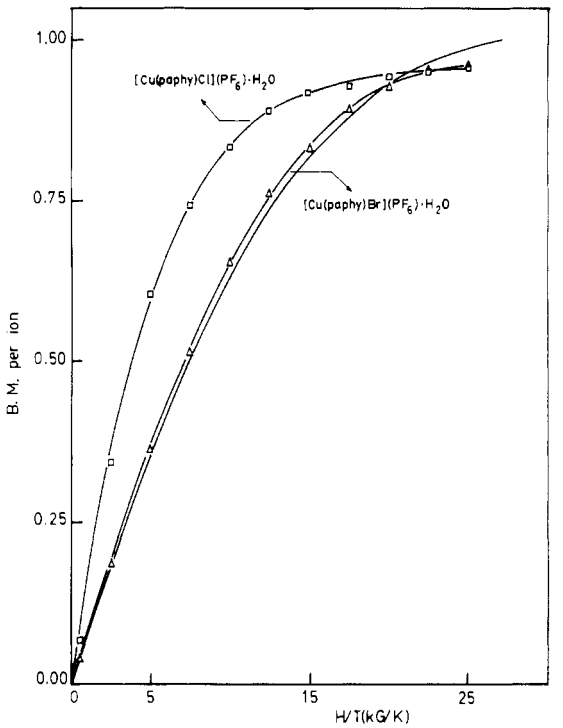

Figure 8. Variation of magnetization with applied magnetic field at $T = 2$ K for the $[Cu(paphy)X](PF_6)\cdot H_2O$ (X = Cl, Br) complexes and for the ideal paramagnetic compound.

where $S = {}^1/_2$, r_K is the distance between the paramagnetic ions, and ϑ is the angle between the vector defined by the positions of these ions and the axis of the applied magnetic field. The sum is restricted to sites of the magnetic ions included in a tridimensional lattice 30 × 30 × 30 Å^3, and the $\langle g\rangle$ value was fixed to 2.13 from the EPR results. The second-moment values thus obtained are $M_{2,\parallel} = 1.66 \times 10^{18}$ Hz^2 and $M_{2,\perp} = 1.84 \times 10^{18}$ Hz^2

(35) Abragam, A.; Bleaney, B. *Resonance Paramagnetique Electronique des Ions de Transition*; Presses Universitaires de France: Paris, 1971; Chapter 9.
(36) (a) Slichter, C. P. *Principles of Magnetic Resonance*; Harper and Row: New York, 1963; Chapter 3. (b) Pake, G. E. *Paramagnetic Resonance*; Benjamin: New York, 1962; Chapter 4.
(37) McGregor, K. T.; Soos, Z. G. *J. Chem. Phys.* **1976**, *64*, 2506.
(38) (a) Willett, R. D.; Jardine, F. H.; Roberts, S. A. *Inorg. Chim. Acta* **1977**, *25*, 97. (b) Landee, C. P.; Lamas, A. C.; Greeney, R. E.; Gahlawat, P. S. *J. Appl. Phys.* **1984**, *55*, 2473.
(39) (a) Watkins, N. T.; Jeter, D. Y.; Hatfield, W. E.; Horner, S. M. *Trans. Faraday Soc.* **1971**, *67*, 2431. (b) Willett, R. D.; K'un Chang. *Inorg. Chim. Acta* **1970**, *4*, 447.
(40) (a) Van Ooijen, J. A. C.; Reedijk, J. *J. Chem. Soc., Dalton Trans.* **1978**, 1170. (b) Lundberg, B. K. S. *Acta Chem. Scand.* **1972**, *26*, 3977.
(41) (a) Endres, H.; Nothe, D.; Rossato, E.; Hatfield, W. E. *Inorg. Chem.* **1984**, *23*, 3467. (b) Endres, H.; Genc, N.; Nothe, D. *Z. Naturforsch., B* **1983**, *38B*, 90.
(42) Bandoli, G.; Biagini, M. C.; Clemente, D. A.; Rizzardi, G. *Inorg. Chim. Acta* **1976**, *20*, 71.
(43) Bream, R. A.; Estes, E. D.; Hodgson, D. J. *Inorg. Chem.* **1975**, *14*, 1672.

Table VIII. Magneto-Structural Parameters in μ-Halo Copper(II) Chains[a]

compd[c]	J, cm^{-1}	R, Å	ϑ, deg	Φ, deg	ϑ/Φ	$\vartheta/2R$	$\vartheta R/\Phi$[b]	Φ/R	ref
$[Cu(dmso)_2Br_2]$	−7.9	2.777	146.1	144.6	1.01	26.3	35.6	52.1	38
$[Cu(dmso)_2Cl_2]$	−6.1	2.702	146.1	144.6	1.01	27.0	36.6	53.5	39
$[Cu(imH)_2Cl_2]$	−2.1	2.751	166.9	117	1.43	30.3	25.5	42.5	40
$[Cu(oaoH_2)Cl_2]$	−1.0	2.776	165.6	95.6	1.73	298	20.8	34.4	41
[Cu(bpca)Br]	−0.8	2.887	165.3	94.0	1.75	28.6	19.7	32.5	7
[Cu(bpca)Cl]	−0.4								7
$[Cu(caf)(OH_2)Cl_2]$	+0.5	2.788	178.8	128.1	1.40	32.1	25.7	45.9	42
$[Cu(paphy)Cl](PF_6)\cdot H_2O$	+0.6	2.805	167.6	102.3	1.64	29.8	21.8	36.4	this work
$[Cu(maep)Cl_2]$	+1.6	2.785	176.0	113.6	1.54	31.6	23.2	40.8	43
$[Cu(paphy)Br](PF_6)\cdot H_2O$	|0.06|	3.358	178.4	81.7	2.18	26.6	13.6	24.3	this work

[a] R = Cu–X′ distance; ϑ = X–Cu–L(trans) angle; Φ = Cu–X–Cu′ angle. [b] Values $\times 10^2$. [c] Abbreviations: dmso = dimethyl sulfoxide; imH = imidazole; $oaoH_2$ = oxamide oxime; bpca = *N*-(2-pyridinylcarbonyl)-2-pyridinecarboximidate; caf = 1,3,7-trimethyl-2,6-purinedione (caffeine); paphy = pyridine-2-carboxaldehyde 2-pyridylhydrazone; maep = 2-(2-methylamino)ethyl)pyridine.

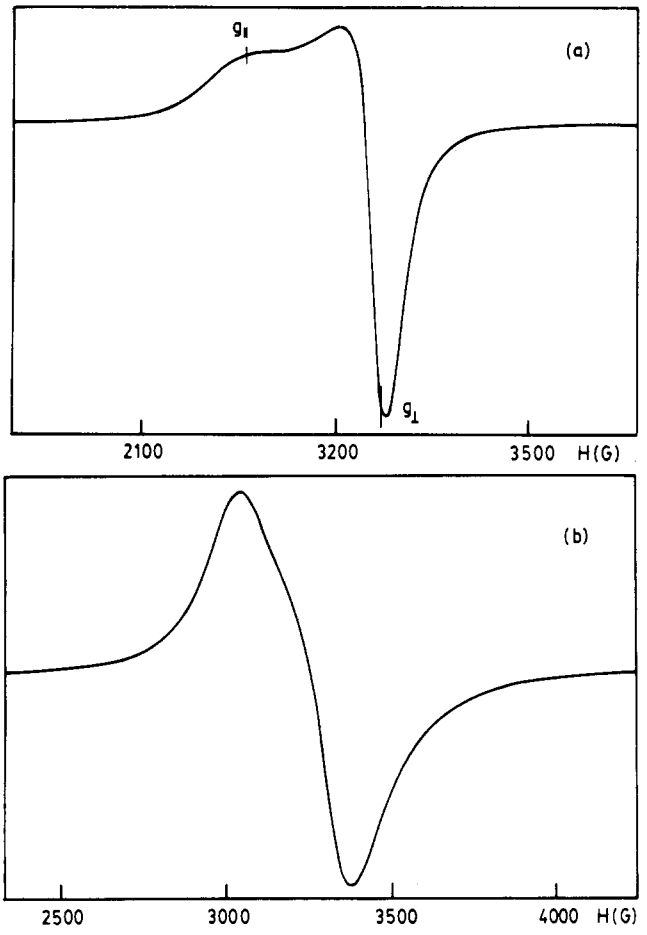

Figure 9. X-Band EPR spectra of a powdered sample of $[Cu(paphy)X](PF_6)\cdot H_2O$ complexes: (a) X = Cl; (b) X = Br.

when the field is, respectively, parallel and perpendicular to the Z axis of the **g** tensor.

In magnetic systems with $J = 0$, the EPR line width is Gaussian with a half-width at half-height of $\Gamma = (2 \ln 2)^{1/2} M_2^{1/2}$.[33-35] In this case, considering the previous second moment values, the $\Gamma_\parallel$ = 1085 G and $\Gamma_\perp$ = 1142 G values calculated would be significantly different from those obtained by the simulation of the experimental EPR spectrum ($\Gamma_\parallel$ = 270 G, $\Gamma_\perp$ = 390 G; see Table VII). These results indicate the presence of a weak magnetic coupling in the ladderlike chain, which reduces the line width. The exchange parameter can be calculated from the equation[35-37] $\Gamma = 2^{1/2} M_2/3J$. The value thus obtained, $|J| = 0.063$ cm^{-1}, agrees satisfactorily with the conclusion obtained from the susceptibility data ($J < 0.1$ cm^{-1}).

Magneto–Structural Correlations. The experimental magnetic data accumulated for such simple systems as parallel square-planar halo-bridged copper(II) dimers have been shown to have only rough dependences on topological parameters.[5] From an inspection of data in Table VIII it is evident that a simple magneto–structural correlation does not exist in the reported compounds. This is not surprising, owing to the large number of possible (and independent) parameters to be considered in these polymeric compounds, when compared with the number in simpler systems.

It can be noted that J values are weak in all cases. This can be understood by taking into account the actual geometry of the entities. In all the cases, the copper(II) orbital ground state $d_{x^2-y^2}$ and the exchange path, involving the d_{z^2} orbital, is very unfavored. Nevertheless, some trends can be reported: the antiferromagnetic coupling is favored when the ϑ angle is smaller than 180° (i.e. copper(II) surrounding geometry going toward trigonal bipyramidal involving a greater contribution of the d_{z^2} orbital to the ground state) as well as when the Φ angle is greater than 90° (increasing of the effective overlapping between the magnetic orbitals). In fact, only the derivatives with small ϑ and large Φ angles show significant antiferromagnetic J values. For the ladderlike chains, it is not possible to perform a magneto–structural study because as far as we are aware, there is no theoretical model that allows us to calculate the exchange parameter values.

Acknowledgment. This work was supported in part by a grant from the European Economic Community, No. ST2J-0164-5-E (CD). J.L.M. thanks the Spanish Ministerio de Educación y Ciencia for a FPI fellowship.

Supplementary Material Available: Tables SI–SV, listing physical properties and parameters of data collection and refinement, atomic coordinates (hydrogen positions) and isotropic equivalent thermal parameters, U_{ij} temperature factors, interatomic distances and angles, and main average planes with distances of atoms to planes and dihedral angles for compounds I and II, and Table SVII, showing the distortion of the coordination polyhedra for the bromo(pyridine-2-carboxaldehyde 2-pyridylhydrazone)copper(II), dibromo[2-(aminomethyl)pyridine]copper(II), dibromo(2-methyl-1,2-diaminopropane)copper(II), hydrazinium trichlorocuprate(II), and dichloro(oxamide dioxime)copper(II) compounds and for the ideal geometries octahedron and trigonal prism (11 pages); Table SVI, listing calculated and observed structure factors for compounds I and II (22 pages). Ordering information is given on any current masthead page.